

# Characterization of Fluorescence Lifetime of Photofrin and Delta-Aminolevulinic Acid Induced Protoporphyrin IX in Living Cells Using Single- and Two-Photon Excitation

Jennifer A. Russell, Kevin R. Diamond, Tony J. Collins, Henry F. Tiedje, Joseph E. Hayward, Thomas J. Farrell, Michael S. Patterson, and Qiyin Fang, *Member, IEEE*

## I. INTRODUCTION

**Abstract**—Photodynamic therapy (PDT) is an effective treatment option for various types of invasive tumors. The efficacy of PDT treatment depends strongly on selective cell uptake and selective excitation of the tumor. The characterization of fluorescence lifetimes of photosensitizers localized inside living cells may provide the basis for further investigation of *in vivo* PDT dosage measurements using time-domain spectroscopy and imaging. In this communication, we investigated the fluorescence lifetime of localized Photofrin and delta-aminolevulinic acid (ALA) induced protoporphyrin IX (PpIX) in living MAT-LyLu (MLL) rat prostate adenocarcinoma cells. The MLL cells were incubated with the photosensitizers, and then treated with light under well-oxygenated conditions using a two-photon fluorescence lifetime imaging microscope (FLIM). Fluorescence lifetime images of these cells were recorded with average lifetimes of  $5.5 \pm 1.2$  ns for Photofrin and  $6.3 \pm 1.2$  ns for ALA-induced PpIX. When localized in cells, the lifetimes of both photosensitizers were found to be significantly shorter than those measured in organic solutions. The result for PpIX is consistent with literature values, while the lifetime of Photofrin is shorter than what has been reported. These results suggest that time-domain methods measuring photosensitizer lifetime changes may be good candidates for *in vivo* PDT dosage monitoring.

**Index Terms**—Delta-aminolevulinic acid (ALA), Photodynamic therapy (PDT), Photofrin, fluorescence, fluorescence lifetime imaging, fluorescence lifetime imaging microscope (FLIM), microscopy, protoporphyrin IX (PpIX), time resolved.

Manuscript received September 13, 2007; revised October 8, 2007. This work was supported in part by the Canadian Institutes of Health Research (CIHR), the Natural Sciences and Engineering Research Council (NSERC), the Canada Research Chairs (CRC), the Ontario Photonics Consortium, and the McMaster Biophotonics Facility.

J. A. Russell is with the School of Biomedical Engineering, McMaster University, Hamilton, ON, L8S 4L8 Canada (e-mail: russelja@mcmaster.ca)

K. R. Diamond, J. E. Hayward, T. J. Farrell and M. S. Patterson are with the Department of Medical Physics and Applied Radiation Sciences, and the Juravinski Cancer Centre, Hamilton, ON, L8V 5C2 Canada (e-mail: kevin.diamond@hrcc.on.ca; joe.hayward@hrcc.on.ca; tom.farrell@hrcc.on.ca; mike.patterson@hrcc.on.ca).

T. J. Collins is with the McMaster Biophotonics Facility and the Department of Biochemistry and Biomedical Sciences, McMaster University, Hamilton, ON, L8S 4L8 Canada (e-mail: tcollins@macbiophotonics.ca).

H. F. Tiedje is with the Brockhouse Institute for Materials Research and the Department of Engineering Physics, McMaster University, Hamilton, ON, L8S 4L8 Canada (e-mail: tiedjeh@mcmaster.ca).

Q. Fang is with the Department of Engineering Physics, McMaster University, Hamilton, ON, L8S 4L8 Canada (e-mail: qiyin.fang@mcmaster.ca).

Digital Object Identifier 10.1109/JSTQE.2007.912896

**P**RESENTLY, common methods of cancer treatment include chemotherapy, radiation therapy, and surgery. Chemotherapy, as a systemic treatment, affects fast-dividing cells in the body whether they are cancerous or healthy, and is well known to cause negative side effects in many patients [1]. Radiation therapy, though more localized, can cause severe adverse side effects as it weakly discriminates between cancerous and healthy tissue. Surgical removal of the tumor is an invasive treatment option, incorporating the usual risks associated with surgery. Depending on the location and nature of the tumor, surgical removal may not even be possible, and it is often followed by radiation or chemotherapy [1]. Photodynamic therapy (PDT), as a new cancer treatment option, allows a higher degree of specificity in targeting malignant and premalignant cells than either chemotherapy or radiation, and is less invasive than surgery. It is known that after a photosensitizing drug has been administered to a patient, it accumulates preferentially in fast-dividing cells such as tumor cells [2], [3]. Laser light corresponding to an absorptive region of the photosensitizer is then applied selectively to the tumor, resulting in the excitation of the photosensitizer, which subsequently excites oxygen to its singlet state. Cell death occurs as a result of the damage caused by the singlet oxygen within the cell. The sparing of normal tissue is enhanced by selectively applying the treatment light only to the tumor [3].

Photofrin and delta-aminolevulinic acid (ALA) induced protoporphyrin IX (PpIX) are two photosensitizers that have been approved for clinical use. Photofrin is currently approved for selected oncology applications, such as partially or completely obstructing esophageal cancer, partially or completely obstructing endobronchial cancer, and nonsmall cell lung cancer [4]. ALA-induced PpIX is, at present, in clinical trials for many applications besides the treatment of the precancerous skin condition actinic keratoses, for which it has already been approved [5]. Photodynamic therapy is most effective when proper dosing is achieved. Drug accumulation, light absorption, and levels of oxygenation, however, differ from patient to patient and between different sites in the same patient [2], which often lead to over- or underdosing. Overdose may cause damage to the surrounding normal tissue while underdose may result in residual dysplasia or malignant tissue. Current dosing guidelines are not patient specific and are defined by empirical values. For example, the

current FDA-approved dosage for Photofrin follows a clinically determined mean dose based on patient body weight of 2 mg/kg, and 200–300 J/cm of excitation light at 630 nm, depending on the application [6]. In order to help regulate dosing, methods for real time monitoring of the photosensitizer concentration in the target tissue [2] and its interactions with elements of the cellular environment are of great practical importance.

While steady-state spectral imaging provides information regarding drug localization [7], it is not a quantitative measure of local drug concentration due to the interference of chromophores and cellular autofluorescence. These problems may be circumvented by the addition of fluorescence lifetime information, which is independent of signal intensity modulation from the aforementioned sources given sufficient signal-to-noise ratio. In addition, changes in the fluorescence lifetime of a photosensitizer can yield much information about the drug's interactions with the cellular environment, such as oxygen and tissue microenvironment [8], [9]. Time-resolved fluorescence has been applied to macroscopic applications in chemical imaging [10], investigation of atherosclerosis [11], and diagnostics of tumors [12]–[14]. These studies suggest that the use of lifetime information not only improves the specificity of fluorescence-based techniques, but also allows a more robust evaluation of *in vivo* data.

Since molecular binding is one of the factors that influences fluorescence lifetime, it is necessary to characterize the lifetime of the photosensitizers when localized in cells. This can be achieved using fluorescence lifetime imaging microscopy (FLIM), which provides spatially resolved lifetime information. Over the past decade, several FLIM techniques have been developed including frequency-domain modulation [10], time-domain scanning using a gated intensifier [15]–[20], 1-D spatial scanning with a streak camera [21], and 3-D raster scanning in space through time-correlated single-photon counting (TCSPC) [22]. So far, FLIM applications are primarily limited to *in vitro* cellular studies with only a few exceptions [13], [23].

The objective of this study is to quantitatively characterize the fluorescence lifetimes of Photofrin and ALA-induced PpIX localized in living cells using a TCSPC-based FLIM system. The fluorescence lifetimes of both photosensitizers in solutions at physiologically relevant concentrations are also measured under single- and two-photon excitations as references. The data will serve as a baseline for future studies using time-domain spectroscopy and imaging technologies for real-time PDT dosimetry.

## II. MATERIALS AND METHODS

### A. Lifetime Measurement of Bulk Solutions

We investigated the fluorescence lifetimes of Photofrin (Axcan Pharma, Inc., Mont-Saint-Hilaire, QC, Canada) and PpIX (Sigma-Aldrich Canada Ltd., Oakville, ON, Canada) dissolved in organic solvent solutions at known concentrations. Photofrin was dissolved in methanol and PpIX was dissolved in dimethyl sulfoxide (DMSO) at concentrations ranging from 0.1 to 10  $\mu$ M. Solutions were mixed in 3 mL low-fluorescence polystyrene cuvettes (CVD-VIS1 S, Ocean Optics, Dunedin,

FL), which were then placed in a cuvette holder. Details of this setup have been reported elsewhere [9], while a different pulsed laser was used in this study. One face of the cuvette holder held a lens-coupled fiber to admit excitation light at 405 nm from a picosecond laser (60 ps FWHM, PLP-01, PicoQuant, Berlin, Germany) operated at 20 MHz. Emitted fluorescence was collected by a lens-coupled fiber on another face of the cuvette, which was oriented at 90° to the excitation light. The light signal passed through a 580 nm longpass filter (Oriel, Stratford, CT) to help avoid collection of side-scattered excitation light before being collected by a photomultiplier tube (PMT) (H5783P-01, Hamamatsu, Hamamatsu City, Japan). The output electrical signal was then amplified by a 26 dB amplifier (HFAC, Becker & Hickel GmbH, Berlin, Germany) and passed through a passive delay generator (TC412 A, Tennesselec, Lenoir City, TN). Data acquisition was achieved via a TCSPC system (SPC-630, Becker & Hickel GmbH). The SPC-630 setup consisted of a constant fraction discriminator (CFD) followed by a time-to-amplitude converter (TAC). The multi-channel analyzer displayed a histogram of fluorescent photon detection times based on the amplitude of the voltages output by the TAC. Decay constants were found by analysis using the Marquardt–Levenberg algorithm [9]. An instrument response function (IRF) was measured by aligning the source and detection fibers (oriented at 180° through the cuvette holder). A time resolution of 200 ps was determined by measuring the FWHM of the IRF.

Further measurements of Photofrin (100  $\mu$ g/mL, in PBS) were performed using a streak camera system (Streak Scope C4334, Hamamatsu, Hamamatsu City, Japan) to examine whether the method of excitation may affect the measured fluorescence lifetime. The schematic of the setup is shown in Fig. 1. Measurements were made under both single-photon excitation around 400 nm, as well as two-photon excitation at 800 nm. Excitation at 800 nm was achieved using a Ti:sapphire laser (Tsunami, Spectral Physics, Mountain View, CA), pulsed at 80 MHz and with an output power of 500 mW. Excitation at 400 nm was obtained by frequency doubling using a BBO ( $\beta$ -BaB<sub>2</sub>O<sub>4</sub>) crystal and a bandpass filter (BG39, Schott, Mainz, Germany) to block the 800 nm light. The output power at 400 nm was 0.015 mW.

The beam from the Ti:sapphire laser was focused onto the cuvette using a 10 $\times$  lens mounted on an *xyz* stage. A light-tight sample box enclosed the cuvette and lens, with an external beam dump to dispose of the unused portion of the beam. When using two-photon excitation at 800 nm, a bandpass filter (KG5, Schott) was placed in the beam path in the collection tube to block the scattered 800 nm light.

Excitation at 405 nm was accomplished with the diode laser pulsing at 1 MHz. There is minimal difference between 400 and 405 nm in the absorption of both drugs and no difference was observed in the results.

### B. Cell Culture

We investigated drug localization and fluorescence lifetimes of Photofrin and ALA-induced PpIX in MAT-LyLu (MLL) rat

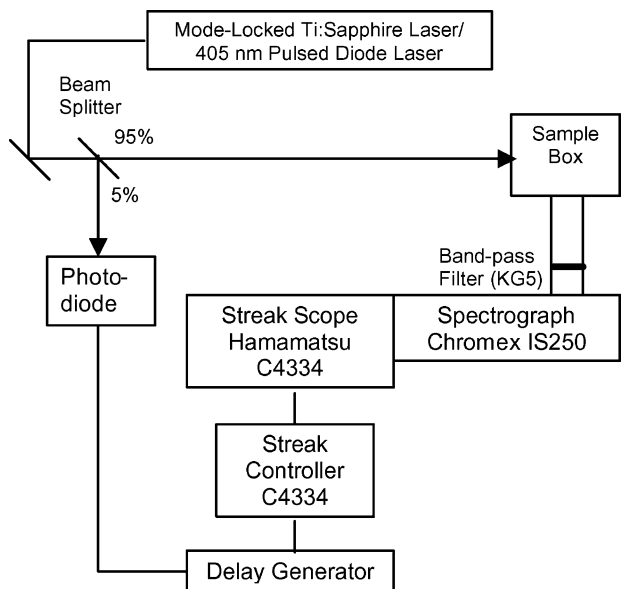


Fig. 1. Streak camera experiment schematic. Excitation was provided by either a mode-locked Ti:sapphire laser pulsing at 80 MHz or a 405 nm diode laser pulsing at 1 MHz. The laser beam was focused at the center of the cuvette placed at the center of a light-tight sample box. The fluorescence emission was collected at  $90^\circ$  to the excitation beam path and focused onto the entrance slit of a spectrograph. The streak camera was placed at the exit focal plane of the spectrograph. A computer workstation was used to control the spectrograph and the streak camera data acquisition.

prostate adenocarcinoma cells *in vitro*, a cell line used in previous studies [24], [25]. These cells were grown in 50 mL vials with 3.5 mL of media and incubated at  $38^\circ\text{C}$  in a water jacketed  $\text{CO}_2$  incubator (Forma Series II, Thermo Fisher Scientific, Inc., Waltham, MA). Media consisted of Roswell Park Memorial Institute (RPMI) medium 1640 (Gibco-BRL, Gaithersburg, MD) supplemented with 10% fetal bovine serum (FBS) (Gibco-BRL), 2% antibiotic/antimycotic (Gibco-BRL) to help protect against contamination, and 1% HEPES buffer to help maintain the pH [24]. For imaging, cells were plated on 25 mm glass coverslips in  $35 \times 10$  mm petri dishes and incubated for a minimum of 6 h to allow attachment before the medium was replaced with medium containing the photosensitizer.

For incubation with Photofrin, a stock solution of 2.5 mg/mL of the photosensitizer dissolved in PBS was prepared and diluted into RPMI medium supplemented with 10% FBS, 2% antibiotic/antimycotic, and 1% HEPES buffer, to a concentration of  $10 \mu\text{g/mL}$  [25]. Cells were incubated in this medium for 18 h before imaging [25].

For incubating with ALA-induced PpIX, the medium was prepared by diluting a stock solution of 96 mM of ALA in DMSO into RPMI medium supplemented with 2% antibiotic/antimycotic and 1% HEPES buffer, to a concentration of 10 mM [24]. Growth medium was removed from the dishes and the cells were rinsed with PBS before the prepared medium was added. Note that the prepared medium did not include FBS, as it interferes with PpIX fluorescence. Cells were incubated in this medium for 4 h before imaging [24].

After incubating for the appropriate time for each photosensitizer, coverslips were rinsed with PBS, placed in a metal bracket

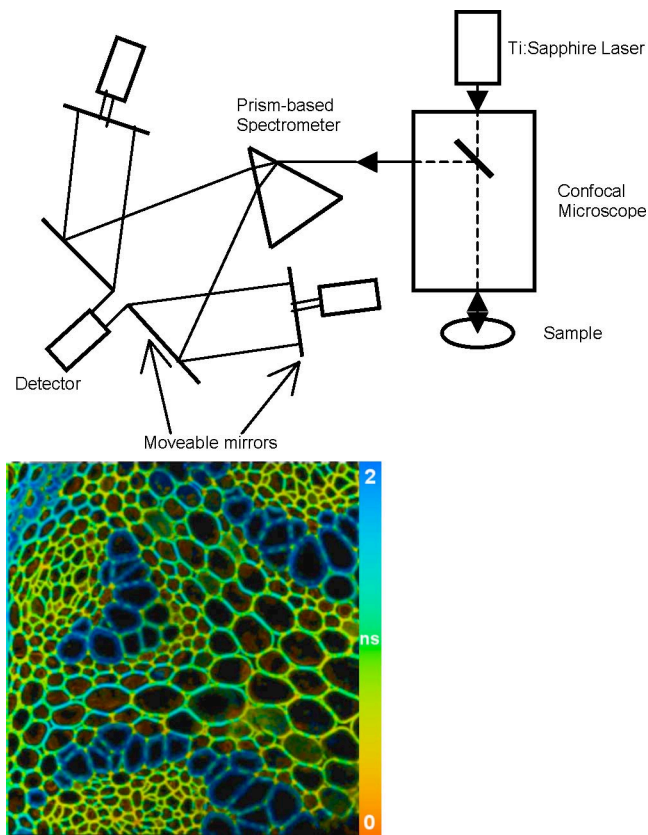


Fig. 2. Schematic for the fluorescence lifetime imaging system (top). The cell sample was excited by a Ti:sapphire laser emitting at 810 nm. Imaging was achieved using a confocal microscope. The emission filter in this system is a prism-based spectrometer that allows for continuous tuning from the near UV to the near IR, with four separate channels and four separate detectors (only three shown here), for simultaneously confocal imaging at four spectral channels. For fluorescence lifetime imaging, only one channel may be active. The light emitted by the sample is dispersed by the prism. The spectrum is sectioned as desired by software-controlled adjustment of the moveable mirrors, and those sections of the spectrum are received by separate detectors. Adapted from Borlinghaus and Kuschel [26]. Fluorescence lifetime image of the rhizome of *Convallaria majalis* taken using this system for spectral and temporal calibration (bottom).

for imaging and bathed in 1 mL PBS to prevent the cells from drying out during imaging.

### C. Fluorescence Lifetime Imaging

Fluorescence lifetime imaging was performed using an inverted multiphoton fluorescence microscope (TSC SP5 & DMI 6000 B, Leica, Wetzlar, Germany), which had an integrated TCSPC-based FLIM module (SPC-830, Becker & Hickel GmbH, Berlin, Germany). FLIM data were analyzed using the built-in software (SPCImage v2.8.3.2921, Becker & Hickel). The schematic of the system is shown in Fig. 2. A Ti:sapphire laser (Chameleon-Ultra, Coherent, Santa Clara, CA, USA) provided two-photon excitation at 810 nm, pulsing at 80 MHz. The emission spectra selection in this system was done through a prism-based spectrometer that allowed continuous tuning from the near UV to the near IR. Emitted fluorescence was monitored over 600–750 nm for collection times of 100, 150 and 300 s for Photofrin-incubated cells, PpIX-incubated cells, and unstained cells, respectively. Confocal and differential

interference contrast (DIC) images were also acquired for each imaged cell group.

### III. RESULTS

#### A. Photosensitizers Dissolved in Organic Solvents

Eleven concentrations of Photofrin (in methanol) and PpIX (in DMSO) ranging from 0.06 to 6  $\mu\text{g/ml}$  and 0.1 to 10  $\mu\text{M}$ , respectively, were measured using the TCSPC system, as described in Section II-A. The data were analyzed using SigmaPlot (Systat Software, Inc., San Jose, CA), which employed a Marquardt–Levenberg-based algorithm that allowed fitting of decays with up to three exponentials and seven parameters. Deconvolution was not necessary as the time resolution of the system (200 ps) was sufficiently small compared to the lifetimes measured.

Photofrin exhibited biexponential decay with an average lifetime of  $10.0 \pm 0.6$  ns. The data were fitted with a biexponential decay calculated using four parameters: amplitude and decay constant for each of the two exponentials. A slow component of  $11.6 \pm 0.5$  ns was retrieved, as well as a fast lifetime component of  $4.8 \pm 0.9$  ns. The slow component likely corresponds to the monomer decay time, which Cubeddu *et al.* measured as 14.7 ns in buffer [28]. The fast component is then likely due to longer polymers, aggregates, or photoproducts. Frequency-domain measurements were also taken using a frequency-domain lifetime spectrometer system (Chronos ISS, Champaign, IL), which also indicated a biexponential decay. Long and short lifetimes of  $10.5 \pm 0.1$  ns and  $3.2 \pm 0.2$  ns were observed, and no concentration dependence was observed over this range. It should be noted that at high concentrations, quenching may occur effectively reducing the lifetime. Conversely, other phenomena can occur at high concentrations, such as dimerization, reabsorption, and reemission, which serve to increase the observed lifetime.

PpIX was found to exhibit monoexponential decay with an average lifetime of  $16.4 \pm 0.2$  ns. Errors indicate one standard deviation from the fitted mean. This compared well with a frequency domain measurement taken using the Chronos system, which measured a fluorescence lifetime of  $16.2 \pm 0.1$  ns. It is also in agreement with the findings of Brancaleon *et al.*, who observed a lifetime of  $16.8 \pm 0.6$  ns in DMSO [27]. Again, no significant concentration dependence was observed over the range investigated.

Additionally, we have performed measurements of Photofrin in methanol solution using the FLIM system and found a biexponential decay, where the fast component of  $3.5 \pm 0.5$  ns and the slow component of  $11.9 \pm 1.1$  ns agree with those found using TCSPC ( $4.8 \pm 0.9$  ns and  $11.6 \pm 0.5$  ns) and the Chronos system ( $3.2 \pm 0.2$  ns and  $10.5 \pm 0.1$  ns).

Since two-photon excitation was being used to excite the photosensitizers when conducting FLIM measurements in cells, it was important to determine whether the fluorescence lifetime would be altered because of two-photon excitation. Therefore, measurements of the fluorescence lifetime of Photofrin in PBS were made using the streak camera system, with single-photon excitation being provided at 400 and 405 nm, as well as two-

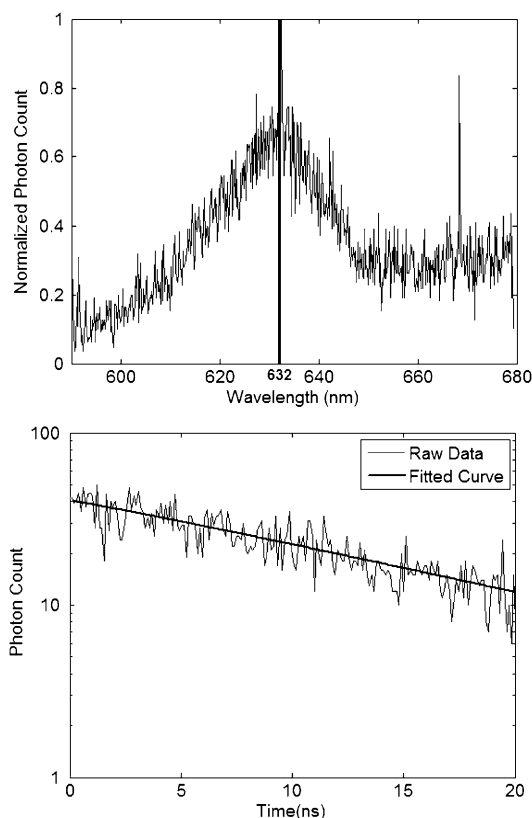


Fig. 3. Emission spectrum for Photofrin measured using the streak camera (top). The broad fluorescence emission peak is centered at 632 nm. Typical fluorescence lifetime decay for Photofrin in PBS at 405 nm excitation, as measured with the streak camera (bottom). An average lifetime of  $13.2 \pm 2$  ns was found.

photon excitation at 800 nm. A summary of the measured lifetimes is shown in Fig. 3. The results exhibited monoexponential decay, fitted using the trust-region algorithm. The average lifetime was measured to be  $13.2 \pm 2.0$  ns, independent of the nature of the excitation.

#### B. Fluorescence Lifetime Imaging in MLL Cells

Fluorescence lifetime images of unstained cells, cells incubated with ALA, and cells incubated with Photofrin were imaged using the multiphoton microscope over the spectral range of 600–750 nm. DIC and steady-state fluorescence images were also taken. The steady-state fluorescence images were acquired at two spectral channels: a green channel from 480 to 570 nm and a red channel from 600 to 750 nm. In unstained cells (see Fig. 4), autofluorescence observed by the green channel is attributed to flavins such as riboflavin, flavin mononucleotide (FMN), and flavin adenine dinucleotide (FAD), which fluoresce around 525 nm. FMN exhibits a fluorescence lifetime of 4.7 ns, while FAD has a lifetime of 2.3 ns [10]. We have measured a fluorescence peak at  $2.6 \pm 0.7$  ns (errors determined from FWHM of the peak in the histogram seen in Fig. 4(c)). The signal collected by the red channel appears to be autofluorescence of the mitochondria, as it was localized in the neighborhood of the nucleus. The fluorescence lifetime distribution histogram for the unstained cells indicated that most cellular autofluorescence

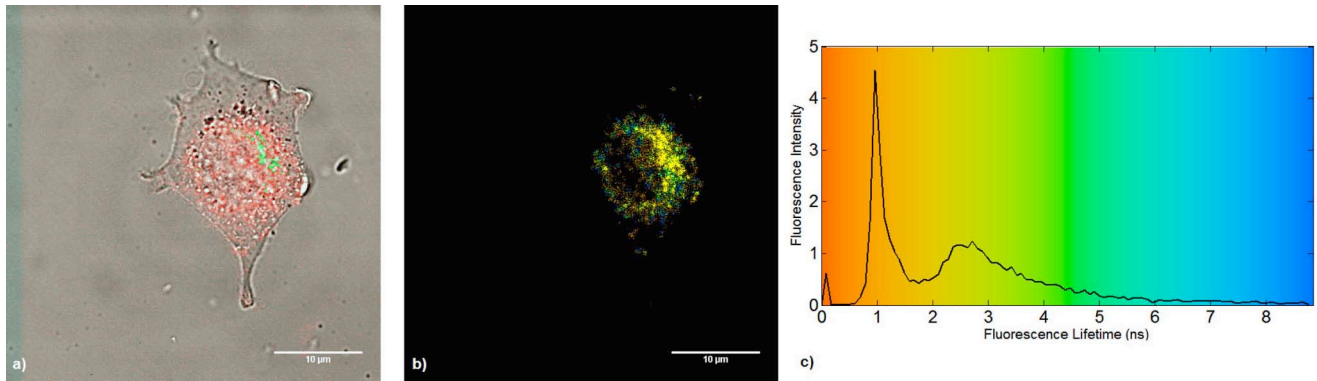


Fig. 4. Unstained cells. (a) Merged steady-state fluorescence-DIC image. Green signal indicates autofluorescence of flavins, and the red signal indicates autofluorescence of the mitochondria. (b) Fluorescence lifetime image. (c) Fluorescence lifetime distribution histogram over the whole image.

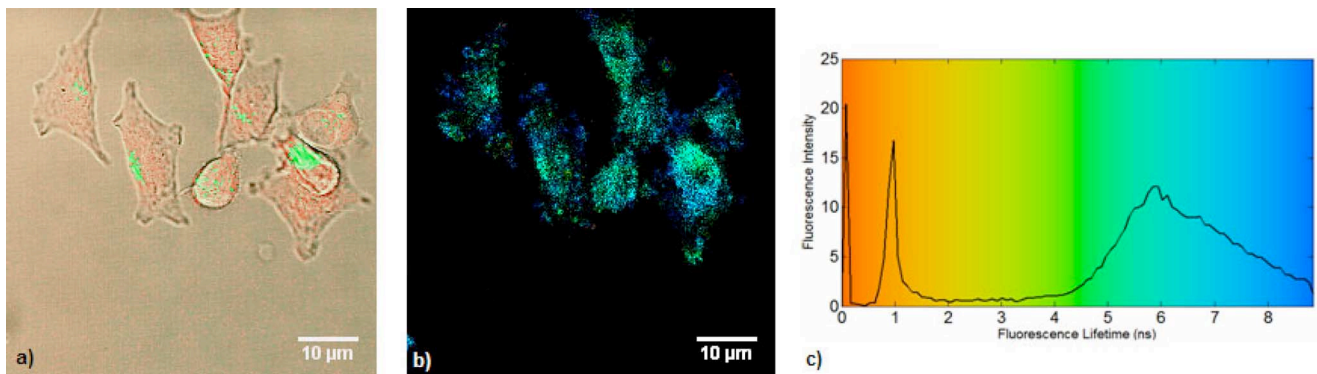


Fig. 5. MLL cells incubated with ALA at  $10 \mu\text{M}$  for 4 h. (a) Merged steady-state fluorescence-DIC image. Green signal indicates flavinoid autofluorescence, and the red signal indicates location of the photosensitizer. Localization of the red signal near the nucleus suggests PpIX accumulation in the mitochondria. (b) Fluorescence lifetime image. (c) Fluorescence lifetime distribution histogram. PpIX exhibited an average lifetime peak of  $6.3 \pm 1.2$  ns.

occurred below 4 ns, as shown in Fig. 4(c). A large peak was observed at  $1.0 \pm 0.1$  ns, which is believed to be autofluorescence attributed mostly to nicotinamide adenine dinucleotide (NADH), which has an emission peak around 460 nm and is known to exhibit a lifetime near 0.3 ns in aqueous buffer, and 1.2 ns when bound to protein [10].

Cells incubated with ALA to induce PpIX were similarly imaged, and were found to exhibit an average lifetime of  $6.3 \pm 1.2$  ns, as seen in Fig. 5. This corresponds to light blue in the false color scheme, as seen on the lifetime histogram. The light blue pixels in the fluorescence lifetime image appear to be colocalized with the red signal in the steady-state DIC image. As with the unstained cells, the red signal in the steady-state-DIC image appears to be located in the neighborhood of the nucleus, indicating that PpIX may be accumulating in the mitochondrial membranes.

Cells incubated with Photofrin were also imaged, and exhibited an average lifetime of  $5.5 \pm 1.2$  ns, as shown in Fig. 6. The pixels corresponding to the photosensitizer in the fluorescence lifetime image again appear colocalized with the red signal of the steady-state fluorescence-DIC image, and again the red signal appeared to be originating in the mitochondria. This would indicate that Photofrin also accumulates in mitochondrial membranes.

The average fluorescence lifetimes exhibited by ALA-induced Photofrin and PpIX in MLL cells were both signifi-

cantly longer than the lifetimes resulting from cellular autofluorescence. This is illustrated in Fig. 7, where the three lifetime histograms appear together, scaled for the NADH autofluorescence that occurs near 1 ns. There is virtually no autofluorescence observed with a lifetime above  $\sim 4$  ns, while the lifetime peaks of the two photosensitizers occur well above 5 ns. It can also be noted that the intensity of the autofluorescence is low compared to the photosensitizers, even at the peak at 2.6 ns. This suggests that the use of time-gated fluorescence for monitoring photodynamic therapy drugs *in vivo* has potential, as interference from tissue autofluorescence will be quite minimal. Additionally, separating the autofluorescence signal and that from the photosensitizer *in vivo* (even though the intrinsic fluorescence is a fraction of the photosensitizer) may improve attempts to quantify the photosensitizer concentration, as a component of a comprehensive model of photodynamic dose.

#### IV. DISCUSSION AND CONCLUSION

We have performed *in vitro* measurements of fluorescence lifetimes of Photofrin and ALA-induced PpIX in living MLL cells using a two-photon FLIM system. The lifetimes of both photosensitizers localized in cells were found to be significantly shorter comparing to the lifetime measured in bulk photosensitizer solutions. The shorter lifetime (6.3 ns) of localized ALA-induced PpIX agrees well with literature values [30]. The

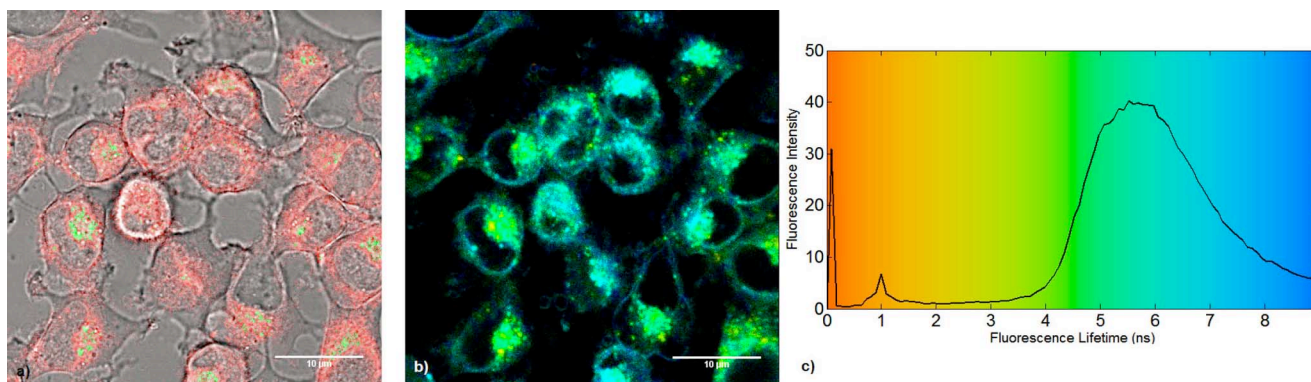


Fig. 6. MLL cells incubated with Photofrin. (a) Merged steady-state fluorescence-DIC image. Green signal indicates flavinoid autofluorescence, and the red signal indicates location of the photosensitizer. Localization of the red signal near the nucleus suggests Photofrin accumulation in the mitochondria. (b) Fluorescence lifetime image. (c) Fluorescence lifetime distribution histogram. Photofrin exhibited an average lifetime peak of  $5.5 \pm 1.2$  ns.

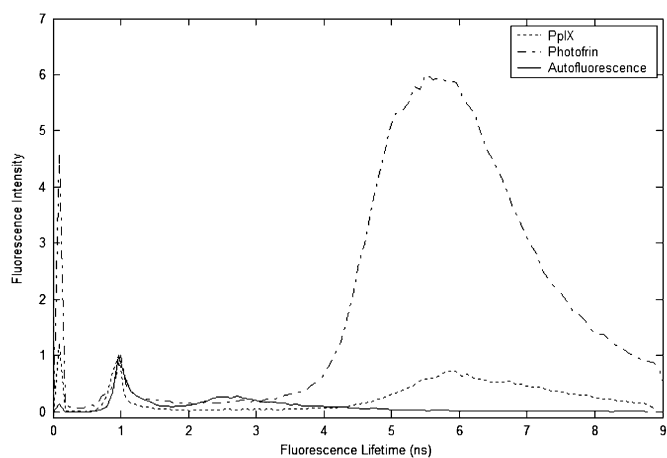


Fig. 7. Fluorescence lifetime distribution histograms for unstained cells (solid), cells incubated with ALA to induce PpIX (dotted) and cells incubated with Photofrin (dot-dashed). Lifetimes of photosensitizers are significantly longer than autofluorescence lifetimes, and above 4 ns autofluorescence is negligible compared to the fluorescence of the photosensitizers.

average lifetime of localized Photofrin (5.5 ns), however, is significantly shorter than what we have previously measured in a cell suspension using TCSPC ( $\sim 13$  ns, data not shown), and is also different from what has been reported in the past [30], [31].

In order to verify the instrumentation and methods used for lifetime measurements, (summarized in Table I) experiments were performed on Photofrin solutions using a streak camera setup and the FLIM system. Both results are consistent with the TCSPC measurements. Our results on FLIM measurements of ALA-induced PpIX in MLL cells confirm the intracellular measurements.

Fluorescence lifetime is a sensitive measure of fluorophore binding and its local environment. Many fluorophores display significantly different fluorescence characteristics when they bind to other molecules. Therefore, FLIM is a useful approach to study localized photosensitizers, as it provides location-specific information compared to traditional measurements of bulk solutions or cellular suspensions.

A study by Ruck *et al.* determined that monomeric Photofrin decayed with an average lifetime of  $13.3 \pm 0.3$  ns in human

TABLE I  
SUMMARY OF LIFETIME MEASUREMENT RESULTS

Lifetime (ns)	PpIX	Photofrin <sup>®</sup>
in Organic Solution Time Domain (Bulk measurement)	$16.4 \pm 0.2$	$10.0 \pm 0.6$ ns $\tau_1: 4.8 \pm 0.9$ $\tau_2: 11.6 \pm 0.5$
in Organic solutions Time Domain (FLIM)		$9.9 \pm 1.2$ ns $\tau_1: 3.5 \pm 0.5$ $\tau_2: 11.9 \pm 1.1$
in Organic Solution Frequency Domain (Chronos)	$16.2 \pm 0.1$	$8.9 \pm 0.1$ ns $\tau_1: 3.2 \pm 0.2$ $\tau_2: 10.5 \pm 0.1$
in Organic Solution Literature Values	$16.8 \pm 0.6$ [27]	14.7 [28]
in MLL Cells (FLIM)	$6.3 \pm 1.2$	$5.5 \pm 1.2$
in Cells Literature Values	$7.44 \pm 0.56$ [29]	monomeric: $13.3 \pm 0.3$ ns [30] $13.2 \pm 2$ ns [31] aggregates: $8.0 \pm 0.6$ ns [30] $1.0 \pm 0.3$ ns [31]

HepG2 cells, while aggregates and photoproducts, which fluoresce at slightly longer wavelengths, decayed with a shorter average lifetime of  $8.0 \pm 0.6$  ns [30]. König *et al.* also documented the formation of Photofrin photoproducts, and found lifetimes of  $13.2 \pm 2$  ns and  $1.0 \pm 0.3$  ns in mice bearing solid subcutaneous Ehrlich carcinoma. The long component was attributed to Photofrin monomers, and the short lifetime to aggregates [31]. Additionally, studies by Schneckenburger *et al.* concerning the fluorescence lifetimes of porphyrins such as Photofrin and a similar compound Photosan in various cell types found three components to the decay; a slow component of 11–14 ns attributed to monomeric porphyrin, a medium component of 2–3 ns attributed to dimers, and a fast component of 0.1–0.3 ns attributed to aggregates [36], [37]. Our results have shown that localized Photofrin fluorescence in cells decays monoexponentially with an average lifetime of  $5.5 \pm 1.2$  ns, significantly different from these reports. It is, however, similar to the change in lifetime between solution and in cells exhibited by ALA-PpIX. Kress *et al.* investigated ALA-induced PpIX in rat epithelial cells, and found a fluorescence lifetime of  $7.44 \pm 0.56$  ns

[29], similar to our results. They also concluded that PpIX was likely accumulated for the most part in the mitochondria [29]. It is likely that the long lifetimes reported previously are the result of measuring the combined contribution from both photoproducts and various types of aggregates. Nevertheless, these variations demonstrated that photosensitizers' lifetimes change significantly when bonded to intracellular components. We speculate that the short lifetime measured in cells for Photofrin may be a result of a high concentration of the drug accumulated in the mitochondria, resulting in self-quenching; however, this hypothesis requires further investigation.

Two-photon excitation holds promise for applications in diagnosis, dosage monitoring, and PDT of small or exact volumes, as is the case with treatment of age-related macular degeneration, which affects the retina [32]. This is largely because the nonlinear interaction is limited to the two-photon excitation volume. This allows treatment volumes on the order of femtolitres, minimizing damage to healthy tissue adjacent to the targeted diseased tissue [32]. The independence of emission spectra on excitation wavelength follows Kasha's rule. Upon excitation into higher vibrational levels, excess energy dissipates nonradiatively, and the fluorophore is left in the lowest vibrational level of the excited state. It is the radiative relaxation from this level that results in fluorescence [10]. Though the one-photon and two-photon absorption spectra may differ, sometimes substantially, for a given fluorophore, the emission spectrum usually does not change [10]. Wilson *et al.* noted that, after internal conversion reduces the fluorophore to the first excited singlet level, photophysical and photochemical processes are identical for one-photon and two-photon excitation [32]. The fluorescence lifetime, hence, does not change with the type of excitation, which is confirmed in our streak camera-based measurements under single- and two-photon excitations.

Ideally, for time-domain measurements, it is desirable to excite the sample with laser pulses that are much farther apart than the lifetime of the sample. In our fluorescence lifetime imaging experiments, an 80 MHz repetition rate excitation was used. In this case, the pulse period of the laser (12.5 ns) was similar to the lifetimes of the photosensitizers being measured. While this would affect the amplitudes for a biexponential fit, it will not influence the measured fluorescence lifetime, as shown in the following. Consider a biexponential decay as

$$y(t) = Ae^{-\frac{t}{B}} + Ce^{-\frac{t}{D}} \quad (1)$$

where  $A$  and  $C$  are the preexponential weightings and  $B$  and  $D$  are the decay constants. Now, consider the resulting decay if  $n y(t)$  decays were overlapped on top of each other with a period of  $\Delta t$  (corresponding to the repetition rate of the laser):

$$y(t) = \left[ Ae^{-\frac{t}{B}} + Ce^{-\frac{t}{D}} \right] + \left[ Ae^{-\frac{t+\Delta t}{B}} + Ce^{-\frac{t+\Delta t}{D}} \right] + \dots + \left[ Ae^{-\frac{t+n\Delta t}{B}} + Ce^{-\frac{t+n\Delta t}{D}} \right]. \quad (2)$$

The exponentials can be separated into exponentials containing only  $-t/\tau$  terms and those containing only factors of  $-\Delta t/\tau$ , where  $\tau$  represents  $B$  or  $D$ . Like terms can then be

collected, giving the following equation:

$$y_n(t) = A \left[ 1 + e^{-\frac{\Delta t}{B}} + \dots + e^{-\frac{n\Delta t}{B}} \right] e^{-\frac{t}{B}} + C \left[ 1 + e^{-\frac{\Delta t}{D}} + \dots + e^{-\frac{n\Delta t}{D}} \right] e^{-\frac{t}{D}} \quad (3)$$

$$y_n(t) = A \left[ \sum_{n=0}^{\infty} e^{-\frac{n\Delta t}{B}} \right] e^{-\frac{t}{B}} + C \left[ \sum_{n=0}^{\infty} e^{-\frac{n\Delta t}{D}} \right] e^{-\frac{t}{D}}. \quad (4)$$

As  $n$  approaches infinity, the sum terms converges asymptotically to constant values. The sum terms are not time dependent, and thus, become a part of the constant term that gives the amplitude for each exponential. The time-dependent terms, however, remain the same as for the original decay expression  $y(t)$ . It should be noted that the previous calculation is based on the assumption that the individual decay dynamics of each pulse remains unchanged. This assumption can be satisfied only if photobleaching and/or other photodynamic processes may be considered insignificant. Therefore, a lower repetition rate and ultrafast source is always desired.

Large differences were seen between the fluorescence lifetimes of the photosensitizers measured in solutions, and those of the photosensitizers measured in cells. Molecular binding is one of the factors that influences fluorescence lifetime. So it is expected that the lifetimes would change depending on the intracellular structures the photosensitizers bound to, e.g., the membranes of the mitochondria.

Fluorescence lifetime imaging with these photosensitizers could also be used for tumor imaging and diagnosis due to the selective uptake of the drugs by malignant tissue. For example, it has been observed that levels of ALA-induced PpIX in normal brain tissue are quite low, and that various factors such as the defective blood-brain barrier and different activity of the heme synthesis pathway contribute to the preferential accumulation of ALA-PpIX in certain brain tumors [33]. Stummer *et al.* assessed the effectiveness of fluorescence-guided resection of malignant gliomas using ALA-induced PpIX, which relies on the sufficient accumulation of fluorescent porphyrins in malignant tissue [34]. The use of Photofrin in fluorescence-guided tumor resection has also been discussed [35]. One limitation of these steady-state fluorescence-based methods is the possible presence of the photosensitizer in surrounding normal tissue, which would result in the resection of healthy tissue. This provides motivation for the characterization of fluorescence lifetimes in cells. König *et al.* determined that significant differences in fluorescence lifetime existed between normal peritumoral tissue and tumor tissue when treated with Photofrin, and resolved that aggregates accumulated preferentially in tumor tissue [31]. Tumor imaging using fluorescence lifetimes could, therefore, provide another level of discrimination between malignant and normal tissue, beyond merely the degree of preferential accumulation.

In summary, Photofrin and ALA-induced PpIX have been imaged using FLIM *in vitro* in MLL cells. Fluorescence lifetimes of both photosensitizers were found to be significantly shorter when localized in cells than when measured in solutions, suggesting that photosensitizers' lifetimes go through significant changes when bonded to intracellular components. Therefore,

one should use caution when interpreting fluorescence lifetime experiment results. On the other hand, these changes in lifetime provide opportunities to quantitatively measure and monitor the binding states of the photosensitizers and their microenvironment, which may be used in real-time PDT dosimetry as well as for diagnosis purposes. From the spatially resolved FLIM images, both photosensitizers appear to be accumulating for the most part in the mitochondria. Colocalization studies have been planned to confirm the localization of both photosensitizers within the cell. Additionally, we plan to investigate the effects of photobleaching and photosensitizer self-quenching on fluorescence lifetime within cells.

#### ACKNOWLEDGMENT

The authors would like to acknowledge Mr. M. Weston from the Department of Medical Physics, McMaster University, for assistance with *in vitro* cell culture experiments; Mr. J. Lovell from the Department of Biochemistry for measuring the absorption–emission spectra and the lifetimes of the two photosensitizers in solution using the frequency domain Chronos system; and Ms. Nanxi Zha from the Department of Electrical and Computer Engineering for her assistance in bibliography search. The cell cultures and fluorescence lifetime imaging measurements were performed at McMaster Biophotonics Facility. They would also like to acknowledge Hamamatsu Corporation, Bridgewater, NJ, for the loan of the streak camera.

#### REFERENCES

- [1] American Cancer Society. (2007, Jan. 7). *Treatment Topics and Resources: Symptoms and Side Effects* [Online]. Available: [www.cancer.org/docroot/mbc/mbc\\_2\\_Side\\_Effects.asp](http://www.cancer.org/docroot/mbc/mbc_2_Side_Effects.asp).
- [2] B. C. Wilson and M. S. Patterson, "The physics of photodynamic therapy," *Phys. Med. Biol.*, vol. 31, no. 4, pp. 327–360, 1986.
- [3] A. Chwilkowska, J. Saczko, T. Modrzycka, A. Marcinkowska, A. Malarska, J. Bielwicz, D. Patalas, and T. Banas, "Uptake of photofrin II, a photosensitizer used in photodynamic therapy, by tumour cells *in vitro*," *Acta Biochim. Pol.*, vol. 50, no. 2, pp. 509–513, 2003.
- [4] G. Williams, R. Pazdur, and R. Temple, "Assessing tumor-related signs and symptoms to support cancer drug approval," *J. Biopharm. Stat.*, vol. 14, no. 1, pp. 5–21, 2004.
- [5] R. Bissonette, A. Bergeron, and Y. Liu, "Large surface photodynamic therapy with aminolevulinic acid: Treatment of actinic keratoses and beyond," *J. Drugs Dermatol.*, vol. 3, no. 1, pp. S26–S31, 2004.
- [6] US Food and Drug Administration: Center for Drug Evaluation and Research. (2007, Jan. 7). *FDA Oncology Tools Product Label Details in Conventional Order for Porfimer Sodium* [Online]. Available: [www.accessdata.fda.gov/scripts/cder/onctools/labels.cfm?GN=porfimer%20sodium](http://www.accessdata.fda.gov/scripts/cder/onctools/labels.cfm?GN=porfimer%20sodium)
- [7] K. R. Diamond, M. S. Patterson, and T. J. Farrell, "Quantification of fluorophore concentration in tissue-simulating media by fluorescence measurements with a single optical fiber," *Appl. Opt.*, vol. 42, no. 13, pp. 2436–2442, 2003.
- [8] M. Schaferling, "Luminescence lifetime-based imaging of sensor arrays for high-throughput screening applications," *Springer Ser. Chem. Sens. Biosens.*, vol. 3, no. 3, pp. 45–92, 2005.
- [9] K. R. Diamond, P. P. Malysz, J. E. Hayward, and M. S. Patterson, "Quantification of fluorophore concentration *in vivo* using two simple fluorescence-based measurement techniques," *J. Biomed. Opt.*, vol. 10, no. 2, pp. 024007-1–024007-10, 2005.
- [10] J. R. Lakowicz, *Principles of Fluorescence Spectroscopy*, 2nd ed. New York: Springer Science/Business Media, 1999.
- [11] J. Tang, F. Zeng, H. Savage, P. P. Ho, and R. R. Alfano, "Laser irradiative tissue probed *in situ* by collagen 380-nm fluorescence imaging," *Lasers Surg. Med.*, vol. 27, pp. 158–164, 2000.
- [12] R. Richards-Kortum and E. Sevick-Muraca, "Quantitative optical spectroscopy for tissue diagnosis," *Annu. Rev. Phys. Chem.*, vol. 47, pp. 555–606, 1996.
- [13] A. Torricelli, A. Pifferi, P. Taroni, E. Glambattistelli, and R. Cubeddu, "In vivo optical characterization of human tissues from 610 to 1010 nm by time-resolved reflectance spectroscopy," *Phys. Med. Biol.*, vol. 46, pp. 2227–2237, 2001.
- [14] J. D. Pitts and M. A. Mycek, "Design and development of a rapid acquisition laser-based fluorometer with simultaneous spectral and temporal resolution," *Rev. Sci. Instrum.*, vol. 72, no. 7, pp. 3061–3072, 2001.
- [15] R. Cubeddu, D. Comelli, C. D'Andrea, P. Taroni, and G. Valentini, "Time-resolved fluorescence imaging in biology and medicine," *J. Phys. D: Appl. Phys.*, vol. 35, pp. R61–R76, 2002.
- [16] K. Dowling, M. J. Dayel, M. J. Lever, P. M. W. French, J. D. Hares, and A. K. L. Dymoke-Bradshaw, "Fluorescence lifetime imaging with picosecond resolution for biomedical applications," *Opt. Lett.*, vol. 23, no. 10, pp. 810–812, 1998.
- [17] J. Siegal, D. S. Elson, S. E. D. Webb, D. Parsons-Karavassilis, S. Leveque-Fort, M. J. Cole, M. J. Lever, P. M. W. French, M. A. A. Neil, R. Juskaity, L. O. Sucharoc, and T. Wilson, "Whole-field five-dimensional fluorescence microscopy combining lifetime and spectral resolution with optical sectioning," *Opt. Lett.*, vol. 26, no. 17, pp. 1338–1340, 2001.
- [18] K. Vishwanath and M. A. Mycek, "Do fluorescence decays remitted from tissues accurately reflect intrinsic fluorophore lifetimes?," *Opt. Lett.*, vol. 29, no. 13, pp. 1512–1514, 2004.
- [19] A. Periasamy, P. Wodnicki, X. F. Wang, S. Kwon, G. W. Gordon, and B. Herman, "Time-resolved fluorescence lifetime imaging microscopy using a picosecond pulsed tunable dye laser system," *Rev. Sci. Instrum.*, vol. 67, no. 10, pp. 3722–3731, 1996.
- [20] Y. Chen and A. Periasamy, "Characterization of two-photon excitation fluorescence lifetime imaging microscopy for protein localization," *Microsc. Res. Technol.*, vol. 63, pp. 72–80, 2004.
- [21] T. Glanzmann, J. P. Ballini, H. Van Der Bergh, and G. Wagnieres, "Time-resolved spectrofluorometer for clinical tissue characterization during endoscopy," *Rev. Sci. Instruments*, vol. 70, no. 10, pp. 4067–4077, 1999.
- [22] A. Egner and S. W. Hell, "Time multiplexing and parallelization in multifocal multiphoton microscopy," *J. Opt. Soc. Amer. A*, vol. 17, no. 7, pp. 1192–1201, 2000.
- [23] D. S. Elson, J. Siegel, S. E. D. Webb, S. Leveque-Fort, D. Parsons-Karavassilis, M. J. Cole, P. M. W. French, and D. M. Davis, "Wide-field fluorescence lifetime imaging with optical sectioning and spectral resolution applied to biological samples," *J. Modern Opt.*, vol. 49, no. 5/6, pp. 985–995, 2002.
- [24] J. S. Dysart and M. S. Patterson, "Photobleaching kinetics, photoproduct formation, and dose estimation during ALA induced PpIX PDT of MLL cells under well oxygenated and hypoxic conditions," *Photochem. Photobiol. Sci.*, vol. 5, pp. 73–81, 2006.
- [25] J. S. Dysart and M. S. Patterson, "Characterization of Photofrin photobleaching for singlet oxygen dose estimation during photodynamic therapy of MLL cells *in vitro*," *Phys. Med. Biol.*, vol. 50, pp. 2597–2616, 2005.
- [26] R. Borlinghaus and L. Kuschel, "Spectral fluorescence lifetime imaging microscopy: New dimensions with Leica TCS SP5," *Nature Methods*, vol. 3, no. 10, pp. iii–iv, Oct. 2006.
- [27] L. Brancaloni, S. W. Magennis, I. D. W. Samuel, E. Namdas, A. Lesar, and H. Moseley, "Characterization of the photoproducts of protoporphyrin IX bound to human serum albumin and immunoglobulin G," *Biophys. Chem.*, vol. 109, pp. 351–360, 2003.
- [28] R. Cubeddu, R. Ramponi, and G. Bottiroli, "Time-resolved fluorescence spectroscopy of hematoporphyrin derivatives in micelles," *Chem. Phys. Lett.*, vol. 109, no. 4, pp. 439–442, 1986.
- [29] M. Kress, T. Meier, R. Steiner, F. Dolp, R. Erdmann, and A. Ruck, "Time-resolved microspectrofluorometry and fluorescence lifetime imaging of photosensitizers using picosecond pulsed diode lasers in laser scanning microscopes," *J. Biomed. Opt.*, vol. 8, no. 1, pp. 26–32, 2003.
- [30] A. Ruck, C. H. Hulshoff, I. Kinzler, W. Becker, and R. Steiner, "SLIM: A new method for molecular imaging," *Microsc. Res. Technol.*, vol. 70, pp. 485–492, 2007.
- [31] K. Konig, H. Wabnitz, and W. Dietel, "Variation in the fluorescence decay properties of haematoporphyrin derivative during its conversion to photoproducts," *J. Photochem. Photobiol. B: Biol.*, vol. 8, pp. 103–111, 1990.

- [32] B. C. Wilson, A. Karotki, M. Khurana, and J. R. Lepock, "Simultaneous two-photon excitation of Photofrin in relation to photodynamic therapy," *Photochem. Photobiol.*, vol. 82, pp. 443–452, 2006.
- [33] A. Bogaards, A. Varma, S. P. Collens, A. Lin, A. Giles, V. X. D. Yang, J. M. Bilbao, L. D. Lilje, P. J. Muller, and B. C. Wilson, "Increased brain tumor resection using fluorescence image guidance in a preclinical model," *Lasers Surg. Med.*, vol. 35, pp. 181–190, 2004.
- [34] W. Stummer, U. Picjmeier, T. Meinel, O. D. Wiestler, F. Zanella, and H. J. Reulen, "Fluorescence-guided surgery with 5-aminolevulinic acid for resection of malignant glioma: A randomised controlled multicentre phase III trial," *Lancet Oncol.*, vol. 7, no. 5, pp. 392–401, 2006.
- [35] V. X. D. Yang, P. J. Muller, P. Herman, and B. C. Wilson, "A multispectral fluorescence imaging system: Design and initial clinical tests in intra-operative photofrin-photodynamic therapy of brain tumors," *Lasers Surg. Med.*, vol. 32, pp. 224–232, 2003.
- [36] H. Schneckeburger, H. Seidlitz, K. Stettmaier, and J. Wessels, "Intracellular polarization, picosecond kinetics and light-induced reactions of photosensitizing porphyrins," *Opt. Eng.*, vol. 31, pp. 1482–1486, 1992.
- [37] H. Schneckeburger, K. König, K. P. Kunzi-Rap, C. Westpal-Frosch, and A. Ruck, "Time-resolved in-vivo fluorescence of photosensitizing porphyrins," *J. Photochem. Photobiol.*, vol. 21, pp. 143–147, 1993.



**Jennifer A. Russell** received the B.Eng. degree in engineering physics from McMaster University, Hamilton, ON, Canada, in 2005, where she is currently working toward the M.A.S. degree in biomedical engineering.

Her current research interests include the areas of optical spectroscopy and applications of fluorescence lifetime information in photodynamic therapy, including new technologies for clinical diagnostics and management of cancer.



**Kevin R. Diamond** received the B.Sc. degree in physics from the University of Waterloo, Waterloo, ON, Canada, in 1998, and the Ph.D. degree in medical physics from McMaster University, Hamilton, ON, Canada, in 2004.

He is currently a Medical Physicist at the Juravinski Cancer Centre, Hamilton. His current research interests include the development of dosimetric tools and techniques for photodynamic therapy, and more generally, diagnostic and therapeutic applications of light.



**Tony J. Collins** received the B.Sc. degree in plant biology in 1992 and the Ph.D. degree in fungal cell biology in 1996 from the University of Edinburgh, Scotland, U.K.

He was a Senior Research Associate in Dr Martin D. Bootman and Prof. Sir Michael J. Berridge's Calcium Signaling Group, Baraham Institute, Cambridge, U.K. He then joined the Wright Cell Imaging Facility, Toronto Western Research Institute, Toronto, ON, Canada. He is currently an Assistant Professor (part time) and the Manager of Mc-

Master Biophotonics Facility, McMaster University, Hamilton, ON. His current research interests include the study of organelle function and dysfunction using live cell imaging techniques.



**Henry F. Tiedje** received the Ph.D. degree in physics from the University of Waterloo, Waterloo, ON, Canada, in 1997.

He is currently a Research Engineer in Brockhouse Institute for Materials Research, McMaster University, Hamilton, ON. His current research interests include terahertz spectroscopy, high-field terahertz pulse generation, and femtosecond pulse characterization.



**Joseph E. Hayward** received the Ph.D. degree in lasers and electro-optics from the Department of Engineering Physics, McMaster University, Hamilton, ON, Canada, in 1993.

He joined the Biomedical Optics Group, Juravinski Cancer Centre, Hamilton, as a Research Associate to assist in the development of optical methods and instrumentation for the diagnosis, staging, and treatment of cancer, as well as the monitoring of cancer treatments. In 1998, he joined the Cancer Centre as a Medical Physicist. He is currently an As-

sistant Professor in the Departments of Radiology and Medical Physics and Applied Radiation Sciences, McMaster University, where he is also an Associate Member of the Department of Engineering Physics. He is also a Member of the Canadian College of Physicists in Medicine, Bethesda, MD. His current research interests include optical methods of monitoring radiation-induced toxicities and noninvasive strategies to identify the margins of malignant skin lesions.



**Thomas J. Farrell** received the Ph.D. degree in medical physics from McMaster University, Hamilton, ON, Canada, in 1990.

He is currently a Medical Physicist at the Juravinski Cancer Centre, Hamilton, and an Associate Professor in the Departments of Radiology and Medical Physics, McMaster University. His current research interests include optical spectroscopy and dosimetry for photodynamic therapy.



**Michael S. Patterson** received the B.Sc. degree from Queen's University, Kingston, ON, Canada, in 1973, the M.Sc. degree from McMaster University, Hamilton, ON, Canada, in 1976, and the Ph.D. degree from the University of Toronto, Toronto, ON, Canada.

He is the Head of medical physics at Juravinski Cancer Centre, Hamilton, ON, Canada, and a Professor in the Department of Radiology and the Department of Medical Physics and Applied Radiation Sciences, McMaster University, Hamilton. His current research interests include photodynamic therapy,

optical diagnostics, and quantitative optical imaging.



**Qiyin Fang** (M'01) received the B.S. degree in physics from Nankai University, Tianjin, China, in 1995, the M.S. degree in applied physics and the Ph.D. degree in biomedical physics from the East Carolina University, Greenville, NC, in 1998 and 2002, respectively.

He was a Staff Research Scientist in Cedars-Sinai Medical Center, Minimally Invasive Surgical Technology Institute, Los Angeles, CA. He is currently an Assistant Professor of engineering physics at McMaster University, Hamilton, ON, Canada, and holds

the Canada Research Chair in biophotonics. His current research interests include optical spectroscopy and image-guided minimally invasive diagnostic and therapeutic devices, miniaturized MOEMS sensors and imaging systems, and advanced optical microscopy and their emerging applications.